Numerical Study on Hydrodynamic Forces for Micro Particle Detachment by Droplet Impact*

Sun Zhenhai[1,2,3,†] and Han Ruijin[2]

(1 *Shanghai Institute of Microsystem and Information Technology, Chinese Academy of Sciences, Shanghai* 200050, *China*)
(2 *Grace Semiconductor Manufacture Corporation, Shanghai* 201203, *China*)
(3 *Graduate University of the Chinese Academy of Sciences, Beijing* 100049, *China*)

Abstract: This paper presents the results of a numerical investigation of micro-sized particle removal by droplet impact. Computational fluid dynamics simulation is used to calculate the flow distribution of droplet impact on a flat surface. The hydrodynamic forces exerted on the particle are then computed. Key factors controlling particle removal are discussed. Both hydrophilic and hydrophobic surfaces are considered. The flow distributions, especially the front edge expanding upon impact at microscale, strongly depend on surface wettability. The associated hydrodynamic forces on the particles vary accordingly. In addition, the impact on a dry surface can produce higher removal efficiency than that on a wet surface. Under the same impact conditions, the drag force exerted on a particle residing on a dry surface can be three orders of magnitudes larger than on a wet surface. Improving droplet impact velocity is more effective than improving droplet size.

Key words: droplet impact; particle removal; drag force; lift force; wettability
PACC: 0340G; 7320H; 7850G
CLC number: TN305.2 **Document code**: A **Article ID**: 0253-4177(2008)06-1081-07

1 Introduction

Preparation of clean silicon surfaces is one of the most important tasks in the semiconductor manufacturing industry. It accounts for more than 20% of the operations and is considered to be a key factor in the final device performance. The shrink of line widths, the increase of wafer sizes, and higher aspect ratios present unprecedented challenges for the control of particulate contaminants and surface roughness. The front end of line (FEOL) critical particle size is expected to decrease to 25nm by 2009[1]. Silicon loss and oxide loss per cleaning step are expected to decrease to 0.04nm by then. Highly diluted chemicals are used during conventional RCA cleaning to minimize the silicon and oxide losses, but it is difficult to remove particles to the extent desirable with such highly diluted chemicals. The smaller the particle, the more difficult it is to remove. In general, the adhesion force consists of the van der Waals force and the electrostatic double-layer force. Qin and Li[2] studied the mechanism of traditional wet chemical cleaning. Both numerical model prediction and experimental data showed the amount of undercut became unacceptable when removing nano-particles using chemical cleaning. Especially for the ultra thin gate oxide pre-cleaning, the roughness caused by chemical etching could induce severe leakage current[3]. In order to enhance particle-removal efficiency, a physical aid such as megasonic agitation is generally employed. Megasonic agitation has been used for many years in wafer cleaning, but acoustic agitation achieving a high particle-removal efficiency of 80% or higher damages the 70nm wide polycrystalline silicon gate structures[4]. Reducing the megasonic power can reduce the megasonic damage to the 70nm structures, but it also reduces the particle-removal efficiency.

With the size of device structures decreasing toward 45nm and below, damage-free cleaning without sacrificing the particle-removal efficiency becomes a more difficult challenge. An alternative physical technique, the mixed water/gas jet spray cleaning technique, has recently been reported. This technique has an advantage over the megasonic technique because it can remove smaller particles due to the greater impact of micro droplets at a high speed. Thus, the spray at a high flow rate (or at high speed) of the carrier gas with no added chemicals can essentially remove all particles on unpatterned wafer surfaces without any material loss caused by chemical etching. However, a water/gas jet spray at a high flow rate can easily cause damage to fragile structures on patterned wafer surfaces. As the flow rate decreases, the degree of damage decreases, but at the same time, the particle-removal efficiency also decreases. In order to remove particles using the mixed liquid/gas jet spray with a low flow rate, additional chemical processes (such as

* Project supported by the Grace Semiconductor Manufacturing Corporation
† Corresponding author. Email: szh000@hotmail.com
Received 21 November 2007, revised manuscript received 13 February 2008

APM or $HF/H_2O_2/H_2O$ mixture) to weaken the particle adhesion by etching silicon oxide under the particles have been proposed. In order to get a fine control of the spray cleaning process, understanding the particle removal mechanism of micro droplet spray is necessary, especially the physical force applied to the particles on wafer surface, which has not been well studied.

There are several studies describing the droplet-wall interaction progression[5~7]. When the droplet size is in the scale of micrometres, it is difficult to study the droplet impact progression experimentally. For the application in spray cleaning, the understanding of hydrodynamic forces on the micro-sized particles plays a key role for cleaning efficiency improvement. In this study, the hydrodynamic forces exerted on particles by droplet impact are evaluated numerically. Computational fluid dynamics (CFD) simulation is used to compute the flow distributions and to calculate associated hydrodynamic forces for particle removal.

2 Particle-surface interaction

When a droplet impacts on a flat rigid surface where a stationary particle resides, there are three potential particle removal mechanisms: lifting, sliding, and rolling. Before going into the details of the particle removal mechanism, let us briefly review the forces acting on a particle. The Derjaguin-Landau-Verwey-Overbeek (DLVO) theory describes the adhesion force of a micro-scaled particle adhering to a surface, which consists of the van der Waals force and the electrostatic double layer force. The van der Waals force is

$$F_{\mathrm{vdw}} = \frac{Ad}{12h^2} \tag{1}$$

where A is the Hamaker constant, d is the diameter of the particle, and h is the separation distance between the particle and the substrate (for smooth surfaces, it is taken as the Lennard-Jones separation distance, 0.4nm)

The above equation does not take into account the adhesion force due to deformation. The deformation between the particle and surface depends on the physical properties of the materials involved. The particle and surface properties determine whether the particle or the surface will deform and what kind of deformation occurs. There are three classic treatments on deformation: DMT (Derjaguin-Muller-Toporov), JKR (Johnson-Kendall-Roberts), and MP (Maugis-Pollock) models. The JKR and DMT models describe the adhesion of an elastically deforming system. The MP model, on the other hand, describes tensile interaction and plastic deformation. In our study, the MP model is applied for the silica/substrate system[8]. Bowling[8] gave the total adhesion force including the component due to the deformation:

$$F_{\mathrm{vdw}} = \frac{Ad}{12h^2}\left(1 + \frac{2a^2}{hd}\right) \tag{2}$$

where a is the contact radius between the deformed particle and the substrate. Additional contact area by deformation makes the adhesion force larger than without deformation.

The electrostatic double layer force is

$$F_{\mathrm{ed}} = \frac{\varepsilon\varepsilon_0 d(\Psi_{\mathrm{s}}^2 + \Psi_{\mathrm{p}}^2)}{4} \times \frac{\kappa \mathrm{e}^{-\kappa h}}{1 - \mathrm{e}^{-2\kappa h}} \times \left[\frac{\Psi_{\mathrm{s}}^2 \Psi_{\mathrm{p}}^2}{\Psi_{\mathrm{s}}^2 + \Psi_{\mathrm{p}}^2} - \mathrm{e}^{-\kappa h}\right] \tag{3}$$

where ε is the medium dielectric constant, ε_0 is the permittivity of free space, Ψ_{s} and Ψ_{p} are the surface potential of the substrate and the particle, d is the particle diameter, h is the separation distance between the particle and the substrate, and κ is the reciprocal double layer thickness[9].

For many micro-scale particle systems, the electrostatic double layer force is much smaller (2 ~ 3 magnitude lower) than the van der Waals force when the particle and surface are in contact[10]. In this paper, we focus on the van der Waals force.

3 Droplet-particle interaction modeling

When an incident droplet impacts on a dry surface, in general, there are two possible outcomes of the post-impact process. At low impact velocities, the droplet may deposit on the surface and form a liquid film; at high impact velocities, the droplet may splash and secondary droplets may form. The droplet impact hydrodynamics has been investigated theoretically and experimentally in the past years (Hartley & Brunskill 1958; Ford & Furmidge 1967; Stow & Stainer 1977; Mao *et al*. 1997; Rioboo *et al*. 2001). Most experimental studies of droplet impact and spreading have been performed using a high-speed camera. For the hydrodynamic force on the adhering micro-sized particle, a numerical approach was made available only for the laminar flow boundary layer. In our study, the droplet impact produces unsteady flow. Forces exerted on the particle cannot be predicted by the empirical expressions used for laminar flow. In this paper, the hydrodynamic forces on the particle are investigated by computational fluid dynamics simulation.

A two-phase flow approach is employed using the FLUENT VOF multiphase model, with the droplet as the liquid phase and the surrounding air as the gas

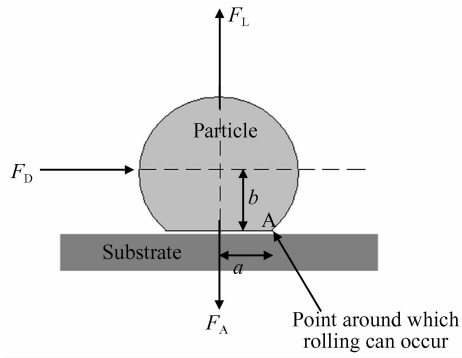

Fig. 1　Forces exerted on the particle when liquid passes over

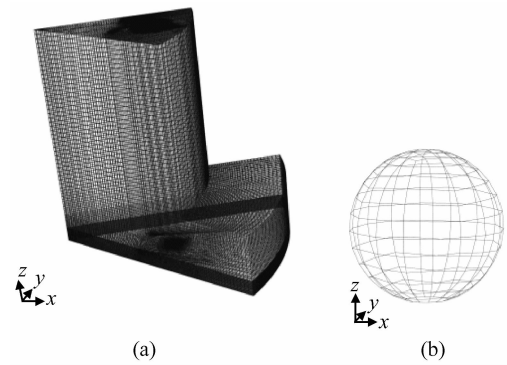

Fig. 2　Computation domain of simulation case and computation mesh on particle　(a) Computation domain; (b) Meshes on particle

phase. The flow field is computed in the unsteady condition under incompressible and isothermal conditions. The liquid droplet is formed by patching the liquid volume fraction with a specified diameter at a specific height from the flat surface. The droplet's initial velocity is also introduced through patching.

The particle on the flat surface is represented by a solid sphere with a specified diameter. The particle is considered as fixed on the flat surface, i. e., the particle trajectory upon impact is not considered. The drag and lift forces exerted on the particle are the hydrodynamic forces in the directions tangential and normal to the surface respectively. Figure 1 shows the forces on the particle, where F_D is the drag force, F_L is the lift force, and F_A represents the adhesion force.

Rolling is the most possible removal model[10]. The rolling criterion can be expressed as

$$M_D + F_D b + F_L a \geqslant F_A a \qquad (4)$$

Equation (4) is derived from a moment balance, where a is the horizontal lever arm, b is the vertical lever arm, and M_D is the moment of surface stress. The lever arm a and b can be calculated according to the MP model. M_D depends on the fluid viscosity, particle size, and flow velocity around the particle. Equation (4) indicates that drag force and lift force play a critical role during the particle removal process.

Flow field distributions from simulation are validated first. Two validations are performed based on the experimental data published by van Dam and Le Clerc[11]. The first set of images were captured when a 85μm droplet impacted a dry hydrophobic surface with a velocity of 5.1m/s. The second set of images were captured when a 66μm droplet impacted a dry hydrophilic surface with a velocity of 11.4m/s. For both cases, a 3D model is constructed. A 45° section of a cylindrical computational domain is shown in Fig. 2. Liquid volume fraction contour plots and video images captured during impact progress are compared in frame-by-frame fashion. The liquid spread ratio, which is defined as $r = d/D_0$ (where d is the liquid spread diameter and D_0 is the droplet initial diameter), is used as the criterion when comparing the numerical results and experimental images. The R square, coefficient of determination, is used to evaluate the goodness of fit curve. The R square of the validation test-1 is 0.97 (Fig. 3 (a) and (b)), while the R

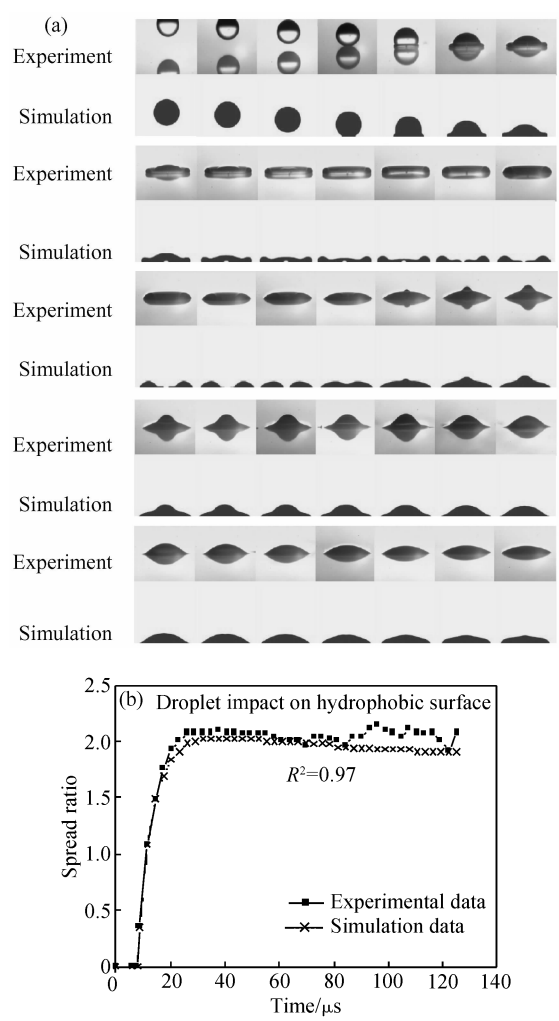

Fig. 3　Model validation one: droplet impact on hydrophobic surface　The time interval between frames is 3μs. Impact condition: droplet size of 85μm, initial velocity of 5.1m/s, static contact angle of 35°.　(a) Frame-by-frame comparison; (b) Spread ratio curve comparison

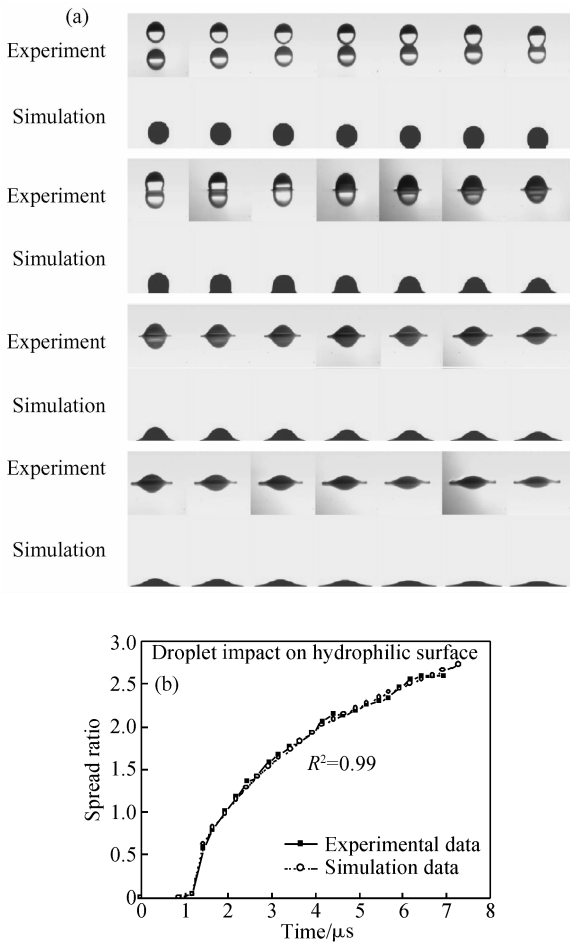

Fig. 4 Model validation two: droplet impact on hydrophilic surface The time interval between frames is 0.25μs. Impact condition: droplet size of 66μm, initial velocity of 11.4m/s, static contact angle of 15°. (a) Frame-by-frame comparison; (b) Spread ratio curve comparison

square of the validation test-2 is 0.99 (Figs. 4 (a) and 4(b)). In both cases, the results show that the simulation model is adequate for the simulation of the droplet impact process on a flat surface.

Once simulation results are validated, numerical DOEs (design of experiments) are carried out. The particle diameter used in all simulations is set at 0.2μm. The simulation matrix is shown in Table 1. The impact position is defined as the distance between the particle and the center of droplet normal projection on flat surface. The wetting property of the surface is specified as hydrophobic and hydrophilic. For the hydrophobic condition, the surface static contact angle is set to 90°. For the hydrophilic condition, a 10° static contact angle is used. In the wet surface cases, we assume that the liquid thickness is 1μm. This is the typical thickness after a 20μm droplet spreads and rests on a flat surface under an initial impact velocity of 50m/s.

Table 1 Simulation case matrix

Droplet size/μm	Droplet velocity/(m/s)	Wetting character	Impact position/μm	Particle size/μm
20	30	Dry/hydrophobic	15	0.2
		Dry/hydrophilic		
		Wet		
	50	Dry/hydrophobic		
		Dry/hydrophilic		
		Wet		
30	30	Wet		

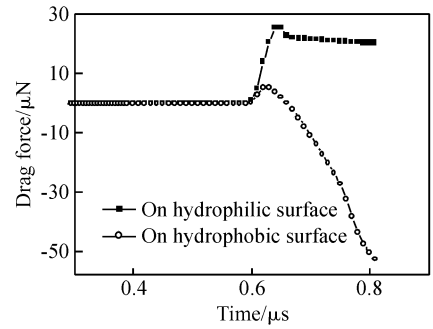

Fig. 5 Drag force on a particle residing on hydrophobic/hydrophilic surface when a 20μm droplet impacts with an initial velocity of 30m/s

The number of computation meshes ranges from 600000 to 900000. The time step used in the computation is 0.001μs. The calculation time ranges from 30 to 100 hours for each case with 4 CPUs on a 64bit Linux Cluster. The time history of forces exerted on the particle after the droplet impact is calculated and extracted.

4 Results and discussion

Because the particle is considered fixed on the surface, particle trajectory is not considered. The drag force and lift force are calculated separately during the whole computation time.

The results of a 20μm droplet impacting on a hydrophobic dry surface show that when the front edge of expanding liquid approaches the particle, the drag force on the particle increases sharply in the liquid spreading direction, then decreases to the negative direction (Fig. 5). The reason for the negative drag force is that for the hydrophobic surface condition, an air packet is formed at the lower side behind the particle due to poor wettability (Fig. 6). The pressure inside the air packet increases with time as a result of compression. For hydrophilic dry surfaces, the force increases sharply as the spreading liquid approaches and stabilizes afterwards. The hydrophilic surface gets wetted quickly so that there is less chance for an air bubble to form behind the particle. Hence, there is no backward pressure force on the particle. The drag forces peak at the same time for these two cases. This is because the computation duration is limited to the

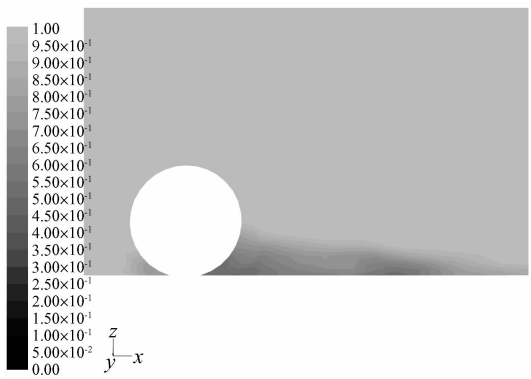

Fig. 6　Liquid volume contour map: air packet behind the particle (0-air, 1-water, flow direction: from left to right)

initial stage of droplet spreading, during which the spreading velocity shows less difference.

The drag forces under different initial droplet impact velocities are also computed and compared. The results of drag forces when a 20μm droplet impacting on a hydrophilic surface with initial velocities of 30 and 50m/s are plotted together in Fig. 7. The drag force of 50m/s is larger than that of 30m/s. This is understandable because high initial velocity produces faster spreading velocity. The drag force is proportional to the liquid velocity spreading over the particle. In addition, the drag force of 50m/s peaks earlier due to its faster spreading velocity.

For wet surfaces, in contrast, the hydrodynamic forces are small. The drag force on a wet surface is about three orders of magnitude smaller than that on a dry surface under the same impact conditions (Fig. 8). On wet surfaces, the droplet momentum transfers to the liquid film first. Through the liquid film, forces are propagated to the particle. While on dry surface, droplet momentum transfers directly to the particle. Thus, when a droplet impacts on dry surfaces, higher removal efficiency can be achieved. For wet surfaces, lift force and drag force are plotted in Fig. 9. Lift force is about two orders of magnitude smaller than drag force. Drag force dominates the detachment of the particle on the wet surface when using droplet impact.

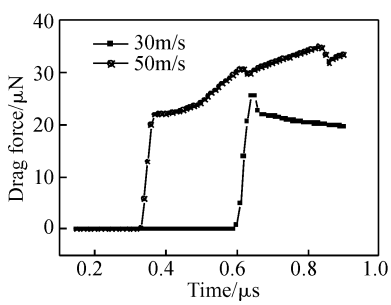

Fig. 7　Drag force comparison between 20μm droplet impacting at 30 and 50m/s

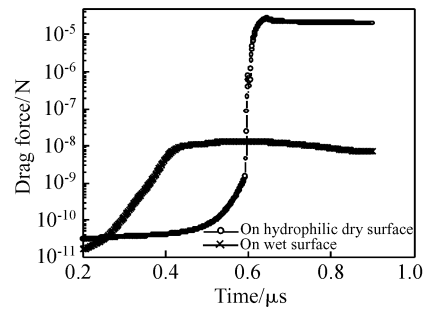

Fig. 8　Drag force comparison between 20μm droplet impacting on dry/wet surface at 30m/s

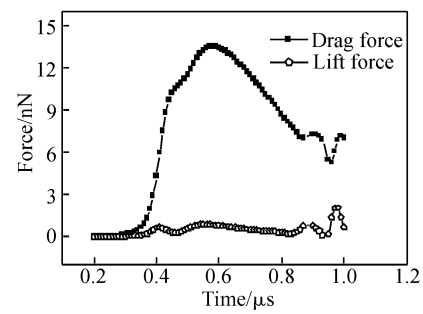

Fig. 9　Drag force and lift force produced by a 20μm droplet impacting on wet surface at 30m/s

The surface is prone to get wet during the actual cleaning process due to multi-droplets spray. So, the drag forces on a wet surface are plotted together (Fig. 9). Different velocities under the same droplet size and different sizes under the same velocity are compared. The peak drag force of a 20μm droplet impacting at 30m/s is 1.35×10^{-8}N; The peak of a 20μm droplet impacting at 50m/s is 2.82×10^{-8}N; The peak of a 30μm droplet impacting at 30m/s is 1.9×10^{-8}N. Drag force increases by 109% when velocity increases from 30 to 50m/s (velocity increases by 67%). On the other hand, drag force increases by 41% when droplet size increase from 20 to 30μm (droplet size increase by 50%). Therefore, improving droplet impacting velocity is more effective than improving droplet size. Small droplets with high impact velocity can produce high particle removal efficiency.

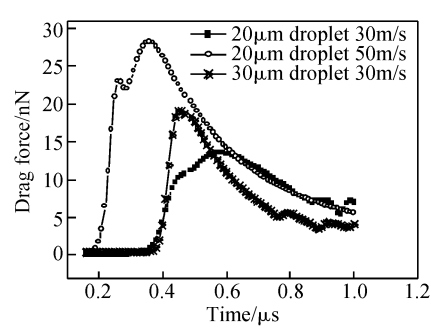

Fig. 10　Drag forces produced by different droplet sizes and initial velocities

According to the results in this study, the hydrodynamic forces produced by droplet impact range from 1×10^{-8} to 4×10^{-5} N. They depend on the droplet impact velocity and surface condition where the particle resides. The forces are also related to the particle size, which is not shown in this paper. In contrast, the adhesion van der Waals force between a 0.2μm SiO_2 particle and a Si surface is in the range of 1×10^{-9} to 3×10^{-8} N (from the literature, the Hamaker constant A ranges from 8.5×10^{-21} to 1.5×10^{-19}). From Eq. (4), the left side of the equation will be much larger than the right side. Particle removal can be achieved. According to practical experiments on spray cleaning, the removal efficiency increases 20%～40% over conventional immersion cleaning[12]. Many researchers studied the removal mechanism by conventional immersion cleaning[2,13]. The undercut etching is necessary to reduce the interaction between the particle and surface. The particle is detached when the electrical repulsive force becomes larger than the adhesion force. On the other hand, no undercut occurs with spray cleaning. Thus, material loss can be avoided. The numerical study of droplet impact can play a key role for the removal efficiency improvement in the implement of spray cleaning in advanced VLSI processes.

5 Summary

The hydrodynamic forces exerted on micro-sized particles by droplet impact are calculated and discussed. For a particle on a dry hydrophobic surface, an air packet forms at the backside of the particle when the front edge of spreading liquid passes over. It induces a reverse direction drag force. When the particle resides on a wet surface, the hydrodynamic drag force is three orders of magnitude smaller than that on dry surface. The faster the impact velocity, the larger the drag force. The drag force is two orders of magnitude larger than the lift force when the particle resides on a wet surface. Thus, the dominant factor of detachment is drag force. Smaller droplets produce smaller drag force. In the cleaning process, there is a tradeoff between the cleaning efficiency and the pattern damage. Cleaning recipes can be optimized through changing droplet sizes and impact velocity according to specific applications.

The hydrodynamic force provided by droplet impact in spray cleaning produces no material loss, while high removal efficiency can be achieved. This study provides numerical evidence of the high efficiency of spray cleaning.

References

[1] International Technology Roadmap for Semiconductors (ITRS), 2004

[2] Qin K, Li Y. Mechanisms of particle removal from silicon surface in wet chemical cleaning process. J Colloid Interface Sci, 2003, 261:569

[3] Zhang J F, Duan Xiaorong, Tan Changhua, et al. The conduction mechanism of stress induced leakage current through ultra-thin gate oxide under constant voltage stresses. Chin Phys, 2005, 14: 1886

[4] Roisman I V, Rioboo R, Tropea C. Normal impact of a liquid drop on a dry surface model for spreading and receding. Proc R Soc Lond, 2002, 458:1411

[5] Rioboo R, Marengo M, Tropea C. Time evolution of liquid drop impact onto solid dry surfaces. Experiments in Fluids 2002, 33: 112

[6] Elyousfi A B A, Chesters A K, Cazebat A M, et al. Approximate solution for the spreading of a droplet on a smooth solid surface. J Colloid Interface Sci, 1998, 207:30

[7] Bowling R A. Particles and surfaces detection, adhesion and removal. New York: Plenum Press, 1988:129

[8] Russel W B, Saville D A, Schowalter W R. Colloidal dispersions. Cambridge: Cambridge University Press, 1989

[9] Burdick G M, Berman N S, Beaudoin S P. Describing hydrodynamic particle removal from surface using the particle Reynolds number. J Nanoparticle Res, 2001, 3:455

[10] Van Dam D B, Le Clerc C. Experimental study of the impact of an ink-jet printed droplet on a solid substrate. Physics of Fluids, 2004, 16(9):3403

[11] Hirano H, Sato K, Osaka T, et al. Damage-free ultradiluted HF/nitrogen jet spray cleaning for particle removal with minimal silicon and oxide loss. Electrochemical and Solid-State Letters, 2006, 9(2):G62

[12] Okorn-Schmidt H F. Characterization of silicon surface preparation processes for advanced gate dielectrics. IBM J Res Develop, 1999, 43(3):351

喷雾清洗中微颗粒受到流体作用力的研究*

孙震海[1,2,3,†]　韩瑞津[2]

（1 中国科学院上海微系统与信息技术研究所，上海　200050）
（2 上海宏力半导体制造有限公司，上海　201203）
（3 中国科学院研究生院，北京　100049）

摘要：对喷雾清洗过程中微颗粒所受到的流体力进行了研究.由于液滴撞击在平面上产生的不稳定流，无法用现有的层流作用力公式来预测颗粒所受到的作用力，本文采用了计算流体力学模拟的方法对流场分布进行了模拟，并且计算颗粒上相应受到的作用力.通过计算结果，讨论了影响颗粒清除效果的关键因素.研究表明，在微米尺度内，平面的可湿性质对液滴展开的初始阶段流场分布有显著影响，从而也大大影响了平面上颗粒所受到的作用力.此外，撞击在干燥表面时，颗粒受到的拖拽力会比撞击到湿表面上时大三个数量级以上.而在湿表面上时，提高撞击速度会比增大液滴大小来得更有效，主导颗粒去除的力为拖拽力.

关键词：液滴撞击；颗粒去除；拽力；升力；可湿性
PACC：0340G；7320H；7850G
中图分类号：TN305.2　　**文献标识码**：A　　**文章编号**：0253-4177(2008)06-1081-07

* 上海宏力半导体制造有限公司资助项目
† 通信作者.Email:szh000@hotmail.com
2007-11-21 收到，2008-02-13 定稿